Spin dynamics of the Ising-like fully anisotropic spin-$\frac{1}{2}$ antiferromagnet in presence of a staggered magnetic field

Asim Kumar Ghosh*
Department of Physics, Jadavpur University, 188 Raja S. C. Mallik Road, Kolkata 700 032, India
(Received 25 June 2009; revised manuscript received 16 October 2009; published 21 December 2009)

We consider a one-dimensional Ising-like fully anisotropic $S=\frac{1}{2}$ Heisenberg antiferromagnetic Hamiltonian and study the dynamics of domain-wall excitations in the presence of a staggered magnetic field, h_x, along the transverse direction. We obtain dynamical spin-correlation functions along the magnetic field, $S^{xx}(q,\omega)$, and perpendicular to it, $S^{yy}(q,\omega)$. It is shown that the line shapes of $S^{xx}(q,\omega)$ and $S^{yy}(q,\omega)$ are purely symmetric at the zone boundary, $q=\frac{\pi}{2}$. It is observed in $S^{xx}(q,\omega)$ for $\pi/2<q<\pi$ that the spectral weight moves toward high-energy side with the increase in h_x. We discuss the relevance of this model to explain the spin dynamics of $CsCoCl_3$ in presence of weak staggered field.

DOI: 10.1103/PhysRevB.80.214418 PACS number(s): 75.10.Pq, 75.50.Ee, 75.60.Ch

I. INTRODUCTION

The spin-$\frac{1}{2}$ Ising-like antiferromagnetic (AFM) chain has been the subject of theoretical studies for quite some time. The spin dynamics of the system are characterized by a picture of propagating domain walls (or solitons). The magnetic compounds $CsCoCl_3$ and $CsCoBr_3$ are good examples of $S=\frac{1}{2}$ Ising-like AFM chains. The simplest exchange interaction Hamiltonian describing these compounds is the $S=\frac{1}{2}$ XXZ Heisenberg model

$$H_{\mathrm{XXZ}} = 2J\sum_i [S_i^z S_{i+1}^z + \epsilon(S_i^x S_{i+1}^x + S_i^y S_{i+1}^y)], \quad 0<\epsilon<1. \quad (1)$$

For very small ϵ, the lowest order ground state of Eq. (1) is the Néel states with a z component of the total spin given by $S_{\mathrm{T}}^z=0$. Villain[1] has calculated the longitudinal correlation function $S^{zz}(q,\omega)$ based on the basis states consisting of a single domain wall and predicted the appearance of a central peak with sharp shoulders. On the other hand, Ishimura and Shiba[2] proposed a picture of domain-wall pair (DWP) states and showed that the propagating DWPs give rise to an excitation continuum around the Ising excitation energy $2J$. The transverse correlation function $S^{xx}(q,\omega)$ exhibits a broad peak around $2J$. The existence of these peaks of $S^{zz}(q,\omega)$ and $S^{xx}(q,\omega)$ has been verified by inelastic neutron-scattering experiments on $CsCoCl_3$ (Refs. 3–5) and $CsCoBr_3$.[6] A significant feature of the spin-wave response of $S^{xx}(q,\omega)$ near the zone center ($q=\pi$) is that the spectral weights are heavily concentrated toward the lower energy region. Nagler *et al.*[6] added a staggered field term of the form $H_S=h\Sigma_i(-1)^i S_i^z$ to the Hamiltonian in Eq. (1), where the staggered field h has two contributions h_o and h_{ic}. The first contribution originates from taking account of the exchange mixing of higher levels with the ground doublet. The second contribution arises from the interchain exchange interactions at low temperatures. The interchain interactions treated in the mean-field approximation, give rise to the staggered field term h_{ic}. The effective Hamiltonian contains both the terms H_{XXZ} and H_S. The staggered field, H_S, splits the broad peak into discrete peaks which is known as Zeeman ladder and observed in Raman scattering on $CsCoCl_3$ and $CsCoBr_3$.[7] However, the observed line shapes of $S^{xx}(q,\omega)$ are quite different from those of the theoretical predictions. Matsubara and Inawashiro[8] have included a weak next-nearest-neighbor (NNN) ferromagnetic (FM) interaction H_{F} in the Hamiltonian H_{XXZ} in Eq. (1)

$$H_{\mathrm{F}} = -2J'\sum_i [S_i^z S_{i+2}^z + \epsilon(S_i^x S_{i+2}^x + S_i^y S_{i+2}^y)]. \quad (2)$$

They have shown the existence of bound states of DWPs as well as the free DWP states and the transverse correlation function $S^{xx}(q,\omega)$ exhibits a sharp peak at lower energy region. The effect of transverse magnetic field on the spin dynamics of this model has been studied by Murao *et al.*[9] and shown that the spectral weight moves toward the low-energy side in $S^{yy}(q,\omega)$ for $\pi/2<q<\pi$ with the increase in the transverse field, while there is no appreciable change in $S^{xx}(q,\omega)$ for all q. Although the proposed form of NNN FM coupling provides a good description of most of the experimental results, the required magnitudes of the NNN exchange $|J'|\sim 0.1|J|$ is unphysically large.[10] Later, Bose *et al.*[11] proposed the Ising-like fully anisotropic Heisenberg AFM Hamiltonian in one dimension and showed that the asymmetric line shapes of $S^{xx}(q,\omega)$ and the bound states of DWPs can be derived. In 2001, Ghosh[12] studied the above model in presence of transverse field and observed its effect on the correlations functions.

In the absence of staggered magnetic field, S_{T}^z is a good quantum number and the eigenvalues of different S_{T}^z having unequal number of DWPs form different energy bands separating by energy $2J$. In the presence of longitudinal magnetic field, h_z, S_{T}^z still is a good quantum number and the eigenvalues within the same value of S_{T}^z as well as the position of the peak of $S^{xx}(q,\omega)$ shift parallel with the increase in h_z. However, S_{T}^z is no longer a good quantum number in presence of a staggered magnetic field h_x and a mixing of states with different S_{T}^z occurs. Thus, eigenvalues as well as eigenstates will be modified by h_x and the characteristics of the spin dynamics will be different.

In this paper, we study the effect of the staggered field, h_x, on the dynamical spin-correlation functions in a fully anisotropic Ising-like $S=\frac{1}{2}$ Heisenberg AFM chain at low temperatures. Dynamical correlation functions $S^{xx}(q,\omega)$ and

$S^{yy}(q,\omega)$ have been derived using the picture of propagating DWPs. Finally, we introduce this model to explain the spin dynamics of $CsCoCl_3$ in presence of weak staggered field. In Sec. II, the theory and the results for the eigenvalues of the DWP continuum and DWP bound states are derived. The dynamical spin-correlation functions $S^{xx}(q,\omega)$ and $S^{yy}(q,\omega)$ are presented in Sec. III. The comparison with the experimental data are available in Sec. IV. Section V contains a discussion of the results obtained.

II. MODEL AND DOMAIN-WALL PAIR STATES

The crystal structure of $CsCoCl_3$ shows that the magnetic Co^{2+} ions are surrounded by trigonally distorted octahedra of Cl^- ions, which is shown in the Fig. 1(a). The octahedra are drawn in blue line. A closer look into the structure reveals that basal planes (black) of the octahedra which also contain the Co^{2+} ions do not lie in the same plane. The different orientation of the successive octahedra essentially leads to a zigzag orientation of the successive basal planes. But the positions of the Co^{2+} ions in the basal planes are such that they form a chain along the c axis (red line). Therefore, it has been proposed, herewith, that this zigzag orientation of the successive Cl octahedra which provide a strong antiferromagnetic superexchange path between adjacent Co^{2+} ions subsequently leads to a fully anisotropic AFM interaction along with a presence of staggered field h_x along the transverse direction [Fig. 1(b)].

The one-dimensional fully anisotropic Ising-like Heisenberg Hamiltonian in the presence of staggered magnetic field is given by

$$H = 2\sum_{i}^{N} [J_x S_i^x S_{i+1}^x + J_y S_i^y S_{i+1}^y + J_z S_i^z S_{i+1}^z] - g_\perp \mu_B H_x \sum_{i}^{N} (-1)^i S_i^x,$$

$$= 2J\sum_{i}^{N} \left[S_i^z S_{i+1}^z + \frac{\epsilon_1}{2}(S_i^+ S_{i+1}^- + S_i^- S_{i+1}^+) + \frac{\epsilon_2}{2}(S_i^+ S_{i+1}^+ + S_i^- S_{i+1}^-) \right] - \frac{h_x}{2}\sum_{i}^{N} (-1)^i (S_i^+ + S_i^-),$$

$$J = J_z, \quad \epsilon_1 = \frac{J_x + J_y}{2J}, \quad \epsilon_2 = \frac{J_x - J_y}{2J},$$

$$h_x = g_\perp \mu_B H_x, \quad \epsilon_1, \ \epsilon_2 \ll 1. \tag{3}$$

H_x is the transverse magnetic field and assume $h_x \ll 2J$. N is the total number of spins. Since we are interested in excitations at low temperatures, we consider low-lying excited states. These states can be obtained from the Néel state by flipping a block of adjacent spins, giving rise to DWP states with $S_T^z = 0$ and ± 1 (Fig. 2). These excitations occur around the Ising energy $2J$ above the ground state.

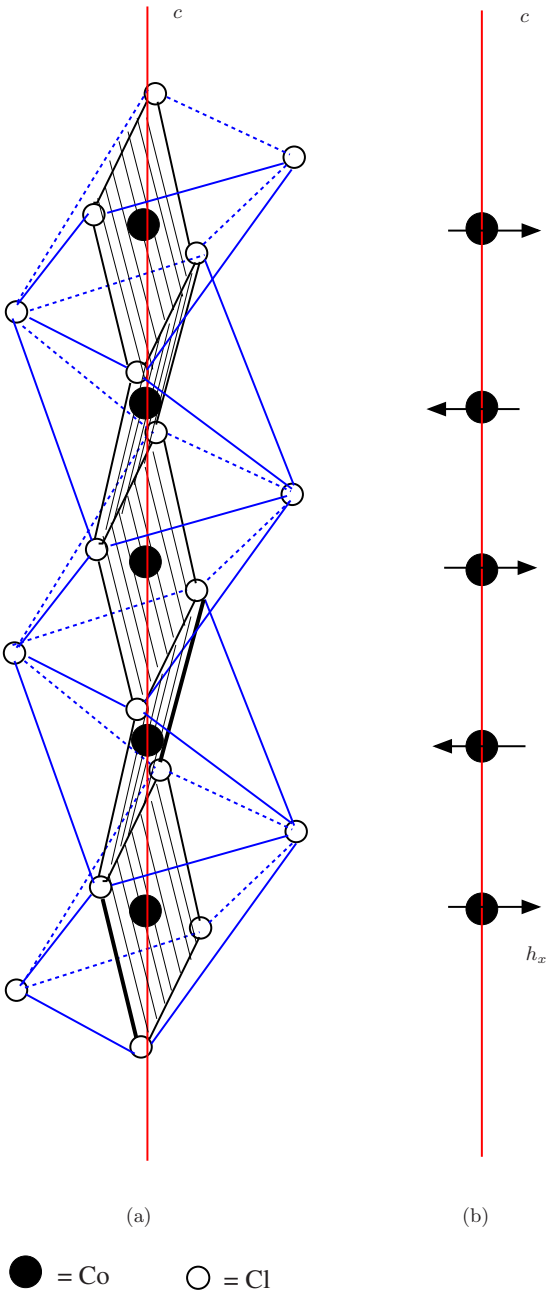

FIG. 1. (Color online) The structure of $CsCoCl_3$ crystal showing the chain of Co^{2+} ions along the c axis (a). The proposed model along with the staggered field on the Co^{2+} ions is shown in (b).

This lowest energy subspace is hereby decoupled into two orthogonal series of states, say, "a" and "b." Series a has been generated by flipping a block of spins which contains j numbers of adjacent spins and the block may begin from any odd (m) site of the $|\text{Néel1}\rangle$ state. Therefore, $\phi_j^{(a)}(m)$ represents that state which contains a block of j number of adjacent flipped spins and this block begins from the mth site. Series a starts from the state with $S_T^z = 1$ where two domain walls are adjacent, i.e., $\phi_1^{(a)}(m)$. The subsequent states $\phi_j^{(a)}(m)(j=2,3,4,\ldots)$ with $S_T^z = 0$ and $+1$ are generated from $\phi_1^{(a)}(m)$ in such a way that the separation between the domain walls is increased by unit lattice distance successively toward the right-hand side of the chain. Hence,

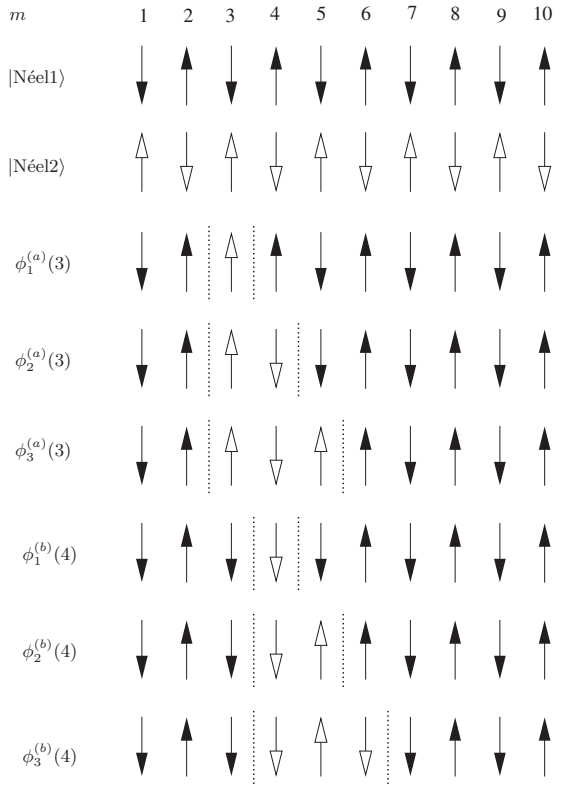

FIG. 2. Néel states and DWP states for $S_T^z = \pm 1$ and 0. The dotted vertical lines indicate the position of domain walls.

$$\phi_1^{(a)}(m) = S_m^+|\text{Néel1}\rangle \quad S_T^z = 1,$$

$$\phi_j^{(a)}(m) = S_{m+j-1}^- \phi_{j-1}^{(a)}(m), (j = 2,4,6,\ldots) \quad S_T^z = 0,$$

$$\phi_j^{(a)}(m) = S_{m+j-1}^+ \phi_{j-1}^{(a)}(m), (j = 3,5,7,\ldots) \quad S_T^z = 1, \tag{4}$$

where $|\text{Néel1}\rangle$ is one of the Néel states. We choose a linear combination of these basis states for describing propagating DWPs with wave vector q as

$$|j,q\rangle_a = \sqrt{\frac{2}{N}} \sum_{m=\text{odd}} e^{-iqm} \phi_j^{(a)}(m). \tag{5}$$

On the other hand, series b has been generated by flipping j numbers of adjacent spins starting from any even (m') site of the $|\text{Néel1}\rangle$ state. Therefore, series b starts from the state with $S_T^z = -1$, i.e., $\phi_1^{(b)}(m')$ and the subsequent states with $S_T^z = 0$ and -1 appear alternately as described below.

$$\phi_1^{(b)}(m') = S_m^-|\text{Néel1}\rangle \quad S_T^z = -1,$$

$$\phi_j^{(b)}(m') = S_{m'+j-1}^+ \phi_{j-1}^{(b)}(m'), (j = 2,4,6,\ldots) \quad S_T^z = 0,$$

$$\phi_j^{(b)}(m') = S_{m'+j-1}^- \phi_{j-1}^{(b)}(m'), (j = 3,5,7,\ldots) \quad S_T^z = -1. \tag{6}$$

Taking a linear combination of these states with wave vector q we have,

$$|j,q\rangle_b = \sqrt{\frac{2}{N}} \sum_{m'=\text{even}} e^{-iqm'} \phi_j^{(b)}(m'). \tag{7}$$

With the help of the Eqs. (5)–(7), one can obtain $H|j,q\rangle_a$ as

$$H|1,q\rangle_a = 2J|1,q\rangle_a + V_{\epsilon_1}|3,q\rangle_a + V_{\epsilon_2}|1,q\rangle_b + \frac{h_x}{2}(|2,q\rangle_a + e^{-iq}|2,q\rangle_b),$$

$$H|2,q\rangle_a = 2J|2,q\rangle_a + V_{\epsilon_1}|4,q\rangle_a + \frac{h_x}{2}(|1,q\rangle_a - |3,q\rangle_a + e^{-iq}|3,q\rangle_b - e^{iq}|1,q\rangle_b),$$

$$\vdots \quad \vdots$$

$$H|j,q\rangle_a = 2J|j,q\rangle_a + V_{\epsilon_1}|j+2,q\rangle_a + V_{\epsilon_1}^*|j-2,q\rangle_a + \frac{h_x}{2}(e^{i\pi j}|j-1,q\rangle_a + e^{i\pi(j+1)}|j+1,q\rangle_a) + \frac{h_x}{2}(e^{-iq}|j+1,q\rangle_b - e^{iq}|j-1,q\rangle_b), \quad j \geq 3, \tag{8}$$

where $V_{\epsilon_1} = \epsilon_1 J(1+e^{-2iq})$ and $V_{\epsilon_2} = 2\epsilon_2 J \cos q$. In the same manner, one could derive similar set of equations for $H|j,q\rangle_b$ in terms of $|n,q\rangle_a$ and $|n,q\rangle_b$.

The Hamiltonian matrix [Eq. (3)] is found to decouple into two orthogonal subspaces, α and β, those are generated after mixing the series a and b in the following way:

$$|j,q\rangle_\alpha = \frac{1}{\sqrt{2}}(|j,q\rangle_a + e^{i\pi(j+1)}|j,q\rangle_b),$$

$$|j,q\rangle_\beta = \frac{1}{\sqrt{2}}(|j,q\rangle_a + e^{i\pi j}|j,q\rangle_b). \tag{9}$$

To distinguish between two series of states, i.e., α and β, the operator $\mathcal{O}$ has been introduced, which is a combination of two operations, spin reversal at every site followed by a translation of one lattice unit. The states $|j,q\rangle_\alpha$ and $|j,q\rangle_\beta$ are found to be the eigenstates of $\mathcal{O}$ having different eigenvalues as mentioned below.

$$\mathcal{O}|j,q\rangle_\alpha = e^{iq}e^{i\pi(j+1)}|j,q\rangle_\alpha,$$

$$\mathcal{O}|j,q\rangle_\beta = e^{iq}e^{i\pi j}|j,q\rangle_\beta.$$

As a result,

$$H|1,q\rangle_\alpha = (2J + V_{\epsilon_2})|1,q\rangle_\alpha + V_{\epsilon_1}|3,q\rangle_\alpha + V_\alpha|2,q\rangle_\alpha,$$

$$H|2,q\rangle_\alpha = 2J|2,q\rangle_\alpha + V_{\epsilon_1}|4,q\rangle_\alpha + (V_\alpha^*|1,q\rangle_\alpha - V_\alpha|3,q\rangle_\alpha),$$

$$\vdots \quad \vdots$$

$$H|j,q\rangle_\alpha = 2J|j,q\rangle_\alpha + V_{\epsilon_1}|j+2,q\rangle_\alpha + V_{\epsilon_1}^*|j-2,q\rangle_\alpha + e^{i\pi j}V_\alpha^*|j-1,q\rangle_\alpha + e^{i\pi(j+1)}V_\alpha|j+1,q\rangle_\alpha, \quad j \geq 3, \tag{10}$$

where $V_\alpha = \frac{h_x}{2}(1-e^{-iq})$. Similarly, one can derive $H|j,q\rangle_\beta$

with α and V_α being replaced by β and $V_\beta = \frac{h_x}{2}(1+e^{-iq})$, respectively. The first excited states can be constructed as a linear combination of the α and β series separately, as described below,

$$\Psi_\alpha(q) = \sum_j \alpha_j |j,q\rangle_\alpha \quad \text{and} \quad \Psi_\beta(q) = \sum_j \beta_j |j,q\rangle_\beta. \quad (11)$$

With the help of the Eq. (10), the following equations for the coefficients $\bar{\alpha}_j$ and $\bar{\beta}_j$ are obtained as:

$$\lambda_{\bar{\alpha}}\bar{\alpha}_1 = (2J + V_{\epsilon_2})\bar{\alpha}_1 + \bar{V}_\alpha \bar{\alpha}_2 + \bar{V}_{\epsilon_1}\bar{\alpha}_3,$$

$$\lambda_{\bar{\alpha}}\bar{\alpha}_2 = 2J\bar{\alpha}_2 + \bar{V}_\alpha(\bar{\alpha}_1 - \bar{\alpha}_3) + \bar{V}_{\epsilon_1}\bar{\alpha}_4,$$

$$\vdots \quad \vdots$$

$$\lambda_{\bar{\alpha}}\bar{\alpha}_j = 2J\bar{\alpha}_j + \bar{V}_\alpha(e^{i\pi j}\bar{\alpha}_{j-1} + e^{i\pi(j+1)}\bar{\alpha}_{j+1}) + \bar{V}_{\epsilon_1}(\bar{\alpha}_{j-2} + \bar{\alpha}_{j+2}), \quad j \geq 3, \quad (12)$$

where $\lambda_{\bar{\alpha}}$ is the eigenvalue, $\bar{V}_\alpha = -h_x \sin(\frac{q}{2})$, $\bar{V}_{\epsilon_1} = -2\epsilon_1 J \cos q$, and $\bar{\alpha}_j = \alpha_j e^{i(q+\pi)/2j}$. In the same manner, one can derive similar set of equations for $\bar{\beta}$ with $\bar{\alpha}$ being replaced by $\bar{\beta}$, $\bar{V}_\alpha$ by $\bar{V}_\beta = h_x \cos(\frac{q}{2})$, $\bar{\alpha}_j$ by $\bar{\beta}_j = \beta_j e^{iq/2j}$ and $\lambda_{\bar{\alpha}}$ by $\lambda_{\bar{\beta}}$, but $\bar{V}_{\epsilon_1} = 2\epsilon_1 J \cos q$.

Dispersion relations are obtained numerically by solving Eq. (12), with $N=2000$. Here, we present the results for $\epsilon_1 = 0.05$ and $\epsilon_2 = 0.10$, since these values are previously estimated in the compound $CsCoCl_3$.[11] Figure 3 shows the dispersion relations for both the $\bar{\alpha}$ and $\bar{\beta}$ series. The spin-wave continuum and the bound-state energy are plotted by dashed and solid lines (red), respectively. In both the series, the bound-state energy always lies above the continuum and the bound state does not exist when $\epsilon_1 > \epsilon_2$. The spectrum for the $\bar{\alpha}$ series is related to that of the $\bar{\beta}$ series by the equation $\bar{\alpha}(q) = \bar{\beta}(q-\pi)$ even in the presence of h_x. When $h_x \neq 0$, the band for the $\bar{\alpha}(\bar{\beta})$ series extends toward the high as well as the low-energy regions resulting a increase in the band width for $\frac{\pi}{2} \leq q \leq \pi (0 \leq q \leq \frac{\pi}{2})$. This feature also enhances with increasing h_x. So, the spin-wave excitations have a finite width at $q = \frac{\pi}{2}$ in contrast with the case of $h_x = 0$. The width also broadens with the increase in h_x. Note that the bound-state energy is not affected by the presence of h_x.

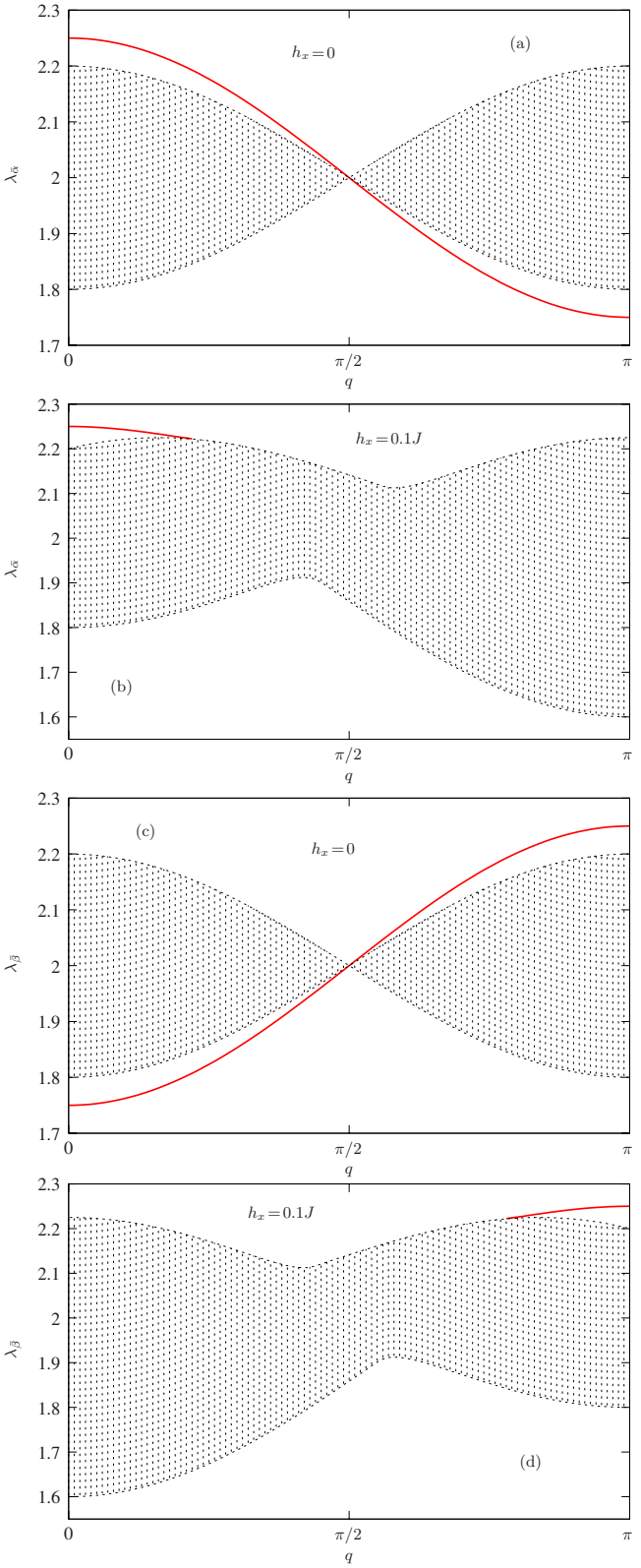

FIG. 3. (Color online) Spin-wave excitation continuum (dashed lines) and DWP bound-state energies (red solid lines) for both the $\bar{\alpha}$ [(a), (b)] and $\bar{\beta}$ [(c), (d)] series, $\epsilon_1 = 0.05$ and $\epsilon_2 = 0.1$.

III. DYNAMICAL SPIN-CORRELATION FUNCTIONS AT $T=0$ K

The dynamical spin-correlation functions along the direction of h_x at $T=0$ is defined as

$$S^{xx}(q,\omega) = \sum_e |\langle \Psi_e | S^x(q) | \Psi_g \rangle|^2 \delta(\omega - \lambda_e + \lambda_g), \quad (13)$$

where $|\Psi_g\rangle$ and $|\Psi_e\rangle$ denote the ground and excited states, respectively, and λ_g, λ_e are the corresponding eigenvalues. In this case, the ground state is the $|\text{Néel}1\rangle$ state and the summation extends over the first excited states only. Also, the Fourier transform of S^x, i.e.,

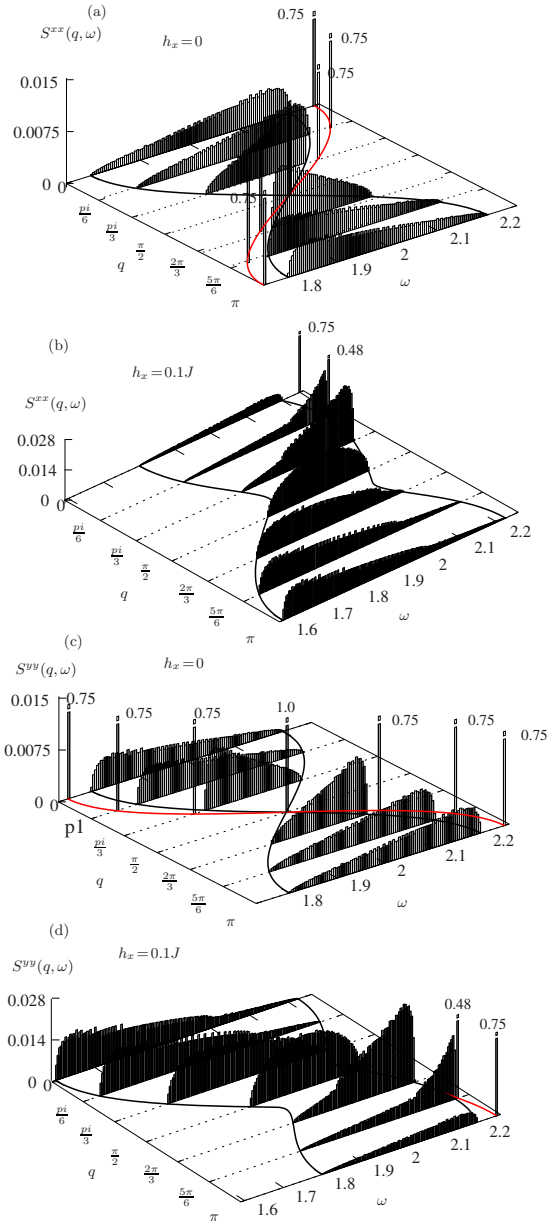

FIG. 4. (Color online) The functions $S^{xx}(q,\omega)$ and $S^{yy}(q,\omega)$ for different values of q for $h_x=0$ [(a), (c)] and $h_x=0.1J$ [(b), (d)]. The width of the histogram is $\Delta\omega=0.004J$.

$$S^x(q) = \frac{1}{2\sqrt{N}}\sum_j e^{iqr_j}(S_j^+ + S_j^-).$$

Similarly, the dynamical spin-correlation function perpendicular to the direction of h_x, $S^{yy}(q,\omega)$, is defined by replacing the superscript x with y in Eq. (13), where

$$S^y(q) = \frac{1}{2i\sqrt{N}}\sum_j e^{iqr_j}(S_j^+ - S_j^-).$$

Since the ground state is the $|\text{Néel1}\rangle$ state, $S^{xx}(q,\omega)$ and $S^{yy}(q,\omega)$ directly reflect the wave-number dependence of the excited states $\Psi_{\bar{\alpha}}(q)=\Sigma_j\alpha_j e^{i(q+\pi)/2j}|j,q\rangle_\alpha$ and $\Psi_{\bar{\beta}}(q)=\Sigma_j\beta_j e^{i\pi/2j}|j,q\rangle_\beta$. With the help of the Eq. (11), the dynamical spin-correlation functions can further be written as[9]

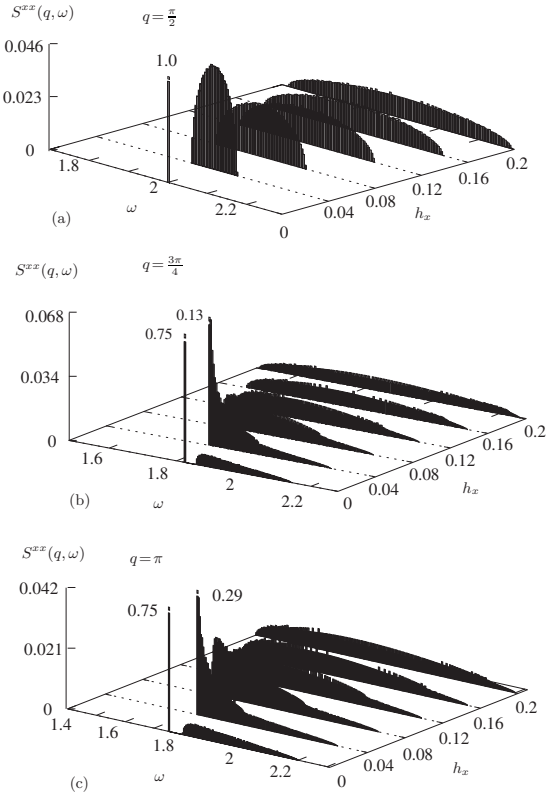

FIG. 5. The function $S^{xx}(q,\omega)$ for different values of h_x with (a) $q=\frac{\pi}{2}$, (b) $q=\frac{3\pi}{4}$, and (c) $q=\pi$. The width of the histogram is $\Delta\omega=0.004J$. $S^{xx}(q,\omega)$ for $q=0$ is not plotted as these line shapes do not change with h_x. Also, $S^{yy}(q,\omega)$ are not shown as they are related to $S^{xx}(q,\omega)$ by the equation $S^{yy}(q,\omega)=S^{xx}(\pi-q,\omega)$.

$$S^{xx}(q,\omega) = \frac{1}{4}\sum_{\bar{\alpha}} |\bar{\alpha}_1|^2\delta(\omega-\lambda_{\bar{\alpha}}+\lambda_g),$$

$$S^{yy}(q,\omega) = \frac{1}{4}\sum_{\bar{\beta}} |\bar{\beta}_1|^2\delta(\omega-\lambda_{\bar{\beta}}+\lambda_g). \quad (14)$$

Note that $S^{xx}(q,\omega)$ depends only on $|\bar{\alpha}_1|^2$ while $S^{yy}(q,\omega)$ on $|\bar{\beta}_1|^2$. Thus, the $\bar{\alpha}$ series contributes on the $S^{xx}(q,\omega)$, whereas the $\bar{\beta}$ series on the $S^{yy}(q,\omega)$. The functions $S^{xx}(q,\omega)$ and $S^{yy}(q,\omega)$ for $h_x=0$ are shown in Fig. 4. The solitary sharp peak originates from the bound state, while the broad peak results from the free DWP states. The intensity of the sharp peak does not depend on the number of spins N, while the broad peak comprises $(N-1)$ peaks of which has intensity on the order of $\frac{1}{N}$. Note that at the zone boundary $(q=\frac{\pi}{2})$, the width of the continuum vanishes. This is also verified in neutron-scattering experiments on $CsCoCl_3$.[4] The line shapes of $S^{xx}(q,\omega)$ for various values of h_x have been plotted in Fig. 5. The main feature of $S^{xx}(q,\omega)$ induced by h_x shows that the line shape is purely symmetric at the zone boundary $(q=\frac{\pi}{2})$ and it is highly asymmetric away from the zone boundary. Since $\bar{V}_\alpha$ vanishes at $q=0$, the shape of $S^{xx}(q=0,\omega)$ is not affected by the presence of h_x. For $\frac{\pi}{2}<q<\pi$, the spectral

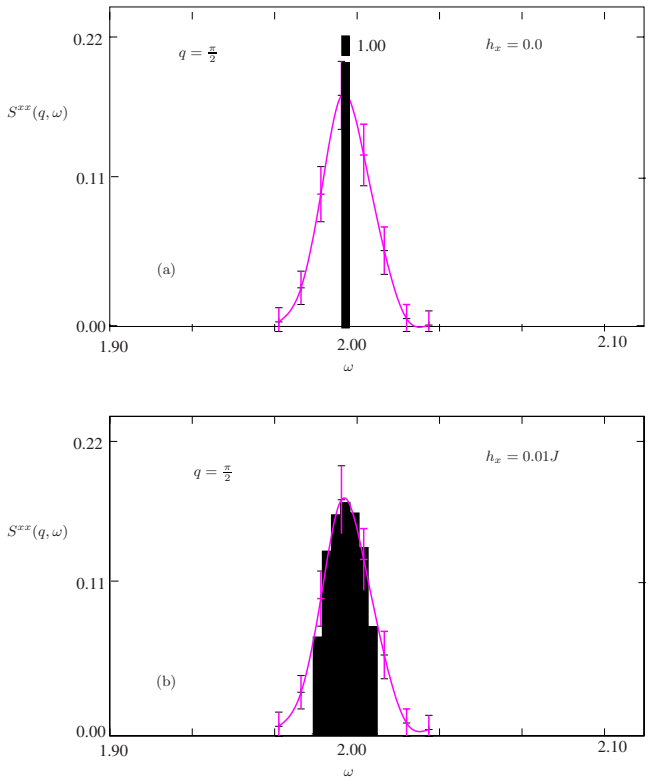

FIG. 6. (Color online) The function $S^{xx}(q,\omega)$, $q=0.5\pi$ for (a) $h_x=0.0$ and (b) $h_x=0.01J$. The width of the histogram $\Delta\omega=0.004J$.

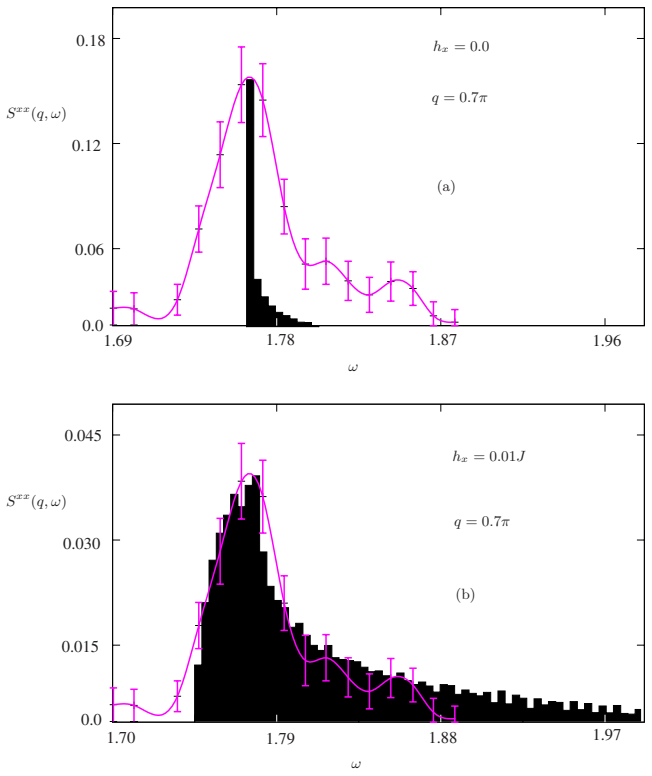

FIG. 7. (Color online) The function $S^{xx}(q,\omega)$, $q=0.7\pi$ for (a) $h_x=0.0$ and (b) $h_x=0.01J$. The width of the histogram $\Delta\omega=0.004J$.

weight concentrates mainly in the low-energy side of the continuum along with the sharp peak. The height of the sharp peak is found to diminish with the increase in h_x. As a result, the spectral weight shifts toward the high-energy side with increasing h_x. So, at higher values of h_x, $S^{xx}(q,\omega)$ tends to regain its symmetric structure even away from the zone boundary. We do not plot the lineshapes of $S^{yy}(q,\omega)$ separately, because $S^{yy}(q,\omega)$ is related to the $S^{xx}(q,\omega)$ by the equation $S^{yy}(q,\omega)=S^{xx}(\pi-q,\omega)$. Note that $S^{xx}(q,\omega)$ for $\frac{\pi}{2}<q<\pi$ and $S^{yy}(q,\omega)$ for $0<q<\frac{\pi}{2}$ are sensitive on h_x as observed by Murao *et al.*[9]

IV. COMPARISON WITH THE EXPERIMENTAL RESULTS

The dynamical structure factors $S^{xx}(q,\omega)$ are plotted in Figs. 6–8 for three different values of the momenta $q=0.5\pi$, 0.7π, and π, separately, and compared with the experimental data obtained by Yoshizawa *et al.*[4] for $CsCoCl_3$. The histograms (black) show the theoretical predictions while the lines with errorbars (magenta) are the experimental results. The functions $S^{xx}(q,\omega)$ with (a) $h_x=0.0$ and (b) $h_x=0.01J$ are plotted separately for better clarity. The figures with the staggered field $h_x=0.01J$ along with $\epsilon_1=0.10$, $\epsilon_2=0.105$ show much better agreement to the experimental results than those obtained with $h_x=0.0$. This observation eventually supports the presence of a staggered magnetic field within $CsCoCl_3$.

V. DISCUSSION OF RESULTS

We have studied the effect of the staggered magnetic field h_x on dynamical properties of one-dimensional fully anisotropic Ising-like antiferromagnet at low temperatures. We have shown using this Hamiltonian that some of the results obtained by Murao *et al.*,[9] in which a FM NNN interaction is

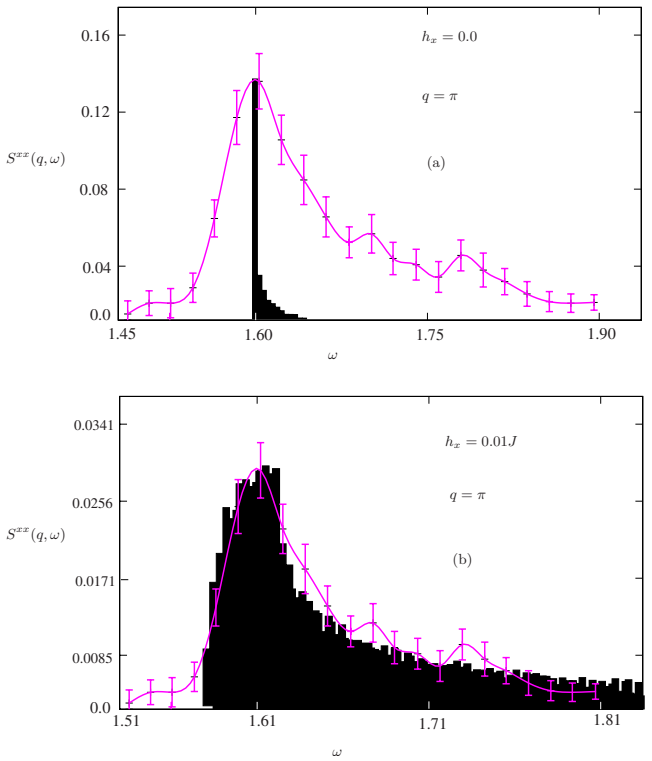

FIG. 8. (Color online) The function $S^{xx}(q,\omega)$, $q=\pi$ for (a) $h_x=0.0$ and (b) $h_x=0.01J$. The width of the histogram $\Delta\omega=0.004J$.

assumed besides the usual AFM NN interaction, can be qualitatively reproduced. These include the formation of DWP bound states, two types of excited modes: $\bar{\alpha}$ and $\bar{\beta}$ and an asymmetry in the line shape of the correlation functions $S^{xx}(q,\omega)$ and $S^{yy}(q,\omega)$. In order to obtain the asymmetry in the line shape of $S^{xx}(q,\omega)$ and $S^{yy}(q,\omega)$, if a FM NNN exchange of magnitude $|J'|\sim 0.1|J|$ is required, which considering that the NNN exchange is through two nonmagnetic ligands would seem to be unphysically large.[10] On the other hand, our model could explain all these characteristics with the usual NN AFM exchange interactions. There are, however, a number of differences. Murao *et al.*[9] observed a single bound-state branch which is symmetric with respect to the zone boundary, whereas in the present study, we obtain asymmetric bound-state branch which always lies above the continuum. No experimental evidence are as yet available on the effect of bound states on the thermodynamic and dynamic properties of the compounds $CsCoCl_3$ and $CsCoBr_3$. The $\bar{\alpha}$ series contribute to $S^{xx}(q,\omega)$, whereas $\bar{\beta}$ series contribute to $S^{yy}(q,\omega)$. Both $S^{xx}(q,\omega)$ and $S^{yy}(q,\omega)$ have symmetry at the zone boundary even in the presence of h_x. This symmetry is totally lost away from the zone boundary. Finally, our theoretical predictions have been compared with the experimental data. An excellent agreement with the experimental results supports the presence of a internal staggered magnetic field within $CsCoCl_3$.

Apart from relevance to experimental system $CsCoCl_3$, the present study is intended to provide insights about the spin dynamics of fully anisotropic Ising-like AFM system in the presence of staggered magnetic field h_x. The ground-state energy and low-lying excitation spectrum of the fully anisotropic Hamiltonian are known exactly because of the mapping between the fully anisotropic Hamiltonian and the exactly solvable eight vertex model.[13,14] The exact results of the fully anisotropic AFM Hamiltonian in presence of a magnetic field in an arbitrary direction are also available,[15] while no exact result is so far available of that model in presence of the staggered field. So, our calculations provide us with some physical insights about spin dynamics in Ising-like fully anisotropic AFM system in presence of the staggered magnetic field.

ACKNOWLEDGMENT

The author, hereby, acknowledges the financial support provided by the Jadavpur University under J. U. Research Grant (Ref. No: P-1/1418/08, dated 01/3.09.2008).

*asimkumar96@yahoo.com

[1] J. Villain, Physica B **79**, 1 (1975).
[2] N. Ishimura and H. Shiba, Prog. Theor. Phys. **63**, 743 (1980).
[3] K. Hirakawa and H. Yoshizawa, J. Phys. Soc. Jpn. **46**, 455 (1979).
[4] H. Yoshizawa, K. Hirakawa, S. K. Satija, and G. Shirane, Phys. Rev. B **23**, 2298 (1981).
[5] J. P. Boucher, L. P. Regnault, J. Rossat-Mignod, Y. Henry, J. Bouillot, and W. G. Stirling, Phys. Rev. B **31**, 3015 (1985).
[6] S. E. Nagler, W. J. L. Buyers, R. L. Armstrong, and B. Briat, Phys. Rev. B **27**, 1784 (1983); **28**, 3873 (1983).
[7] W. P. Lehmann, W. Breitling, and R. Weber, J. Phys. C **14**, 4655 (1981).
[8] F. Matsubara and S. Inawashiro, Phys. Rev. B **43**, 796 (1991).
[9] K. Murao, F. Matsubara, and S. Inawashiro, J. Phys. Soc. Jpn. **64**, 275 (1995).
[10] J. P. Goff, D. A. Tennant, and S. E. Nagler, Phys. Rev. B **52**, 15992 (1995).
[11] I. Bose and A. Ghosh, J. Phys.: Condens. Matter **8**, 351 (1996).
[12] A. Ghosh, J. Phys.: Condens. Matter **13**, 5205 (2001).
[13] J. D. Johnson, S. Krinsky, and B. M. McCoy, Phys. Rev. A **8**, 2526 (1973).
[14] R. J. Baxter, Ann. Phys. (N.Y.) **70**, 323 (1972).
[15] J. Kurmann, H. Thomas, and G. Müller, Physica A **112**, 235 (1982).